Journal of Material Sciences & Engineering

Review Article **Open Access**

Laser Cladding and Thermal Spray Coatings on Steel Pipe Serving the Oil and Gas Industry

Almeida NC[1], Candido LC[1], Faria GL[1], Fernandes de Lima MS[1,2] and Trindade VB[1]*

[1]Redemat/Federal University of Ouro Preto – Brazil
[2]ITA – São Jose dos Campos – Brazil

Abstract

Different coating systems were characterized using a commercial API 5CT steel grade L80 type 1, which is commonly used in the oil and gas industry. Two Ni-based alloys and one Co-based alloy were deposited by laser cladding. Two coatings were deposited (Ni-based alloy and a composite W-C/Co-base) by means of thermal spray process. It has been shown the presence of a hard heat affected zone (HAZ) in the substrate for the as-laser deposited coating. The main explanation for this HAZ is devoted to the heat gradient causing a gradient on the prior austenite grain size and consequently different martensite hardness along the HAZ. For the thermal sprayed coatings, no HAZ was formed due to low heat input process. All the studied coating systems seem to be very interesting for different technically demanding applications, such as, stress sulfide corrosion and wear resistance.

Keywords: Laser cladding; Thermal spray coating; Inconel 625; Hastealloy; Stellite 6; Composite W-C/Co-based alloy

Introduction

In the petroleum industry the application of piping is mandatory in many part of the project for the production of oil and gas (upstream) as well as transportation and refining (downstream). Common materials used to produce those pipes are C-Mn steels. However, there are some parts of the project that C-Mn steels are not complying with the project requirements, mainly regarding corrosion due to CO_2, H_2S, chlorides, etc. [1] as well as strong wear and elevated temperature in some cases [2-5]. Therefore, most noble materials are demanded, such as austenitic steels, super alloys and/or composites ultra-high resistant materials. On the other hand, the manufacture of the entire pipe body using those noble materials can affect strongly the cost, since these materials are very expensive compared to C-Mn steels. Therefore, a possible solution is to develop appropriate coatings using these noble materials on surface of C-Mn steel pipes. Thermal spraying is widely used to provide corrosion protection to ferrous metals or to change the surface properties of the sprayed items, such as improve the wear resistance or thermal conductivity. Thermal spray is defined as applying these coatings takes place by means of special devices/systems through which melted or molten spray material is propelled at high speed onto a cleaned and prepared component surface.

Basically, there are two methods of pipe coating by cladding [6,7]: (i) mechanical or (ii) metallurgical cladding. By mechanical cladding there is no melting of the substrate (base material), which does not cause any metallurgical change in the coating/substrate interface and consequently there is no heat affected zone (HAZ). The bonding is done just by mechanical adherence between the two materials. On the other hand, by metallurgical cladding, such as welding, there are melting of the deposit material and parts of the substrate. This causes a thermal gradient in the substrate, thus affecting its microstructure and properties. The bonding between the two materials happens with metallurgical transformation in the interface coating/substrate.

It is well known in the literature the good performance of Ni-based alloys such as Inconel 625 and C276 alloy (Haste alloy) as well as Co-based alloys with respect to corrosion resistance [8-10]. Furthermore, there are significant amount of contribution regarding the laser cladding of Ni-based alloys and Co-based alloys [11-20]. An alloy such as WC/

Co-base is mainly deposited by thermal spray process as described elsewhere [21-24].

The objective of this present study is to focus on the coating of a commercial steel grade type API 5CT grade L80 type 1 using two Ni-based alloys (Inconel 625 and C276) and one Co-based alloy (Stellite) by means of laser cladding. Additionally, it was investigated two coatings obtained by the thermal spray technique (Inconel 625 and composite W-C/Co-alloy). Microstructural characterization, microhardness measurements of the coatings and of the HAZ were done and discussed.

Materials and Experimental Procedure

The material used for this study is a seamless steel pipe, with outside diameter=244.5 mm and wall thickness=13.84 mm, hot rolled followed by quenching and tempering heat treatment. The chemical composition and the basic mechanical properties are shown in Tables 1 and 2, respectively. The tempering temperature to achieve the API5CT grade L80 type 1 was 650°C and the soaking time was 20 min.

Five different coating systems were used is this study as follows: (i) Co-based alloy – Stellite 6, (ii) Hastealloy – C276, (iii) Inconel 625 alloy and (iv) composite of W-C/Co-based alloy.

C	Mn	Mo	Ni	Si	Ti	Al	Cr	B
0.25	1.05	0.06	0.10	0.20	0.030	0.025	0.35	0.0016

Table 1: Chemical composition (wt.%) of the steel used (Fe is the balance).

Yield strength [MPa]	Ultimate tensile strength [MPa]	Maximum Elongation [%]	Hardness [HV1]	Impact energy at 0°C [J]
615	721	26	220-230	160

Table 2: Basic mechanical properties of the steel used (API 5CT grade L80 type 1).

*Corresponding author: Trindade VB, Redemat/Federal University of Ouro Preto, Brazil, Tel: 31 35591324; E-mail: vicentebraz@yahoo.com.br

The depositions of those coatings were performed through two different processes: (i) laser deposition for all alloys, except the composite W-C/Co-based alloy and (ii) thermal spraying deposition for the Inconel 625 and the composite W-C/Co-based alloy.

The laser deposition was performed using a longitudinal speed of 240 mm/min and laser power of 10 kW. The gas used in the thermal spraying process was oxygen and acetylene and the alloy powders were injected in the formed blame.
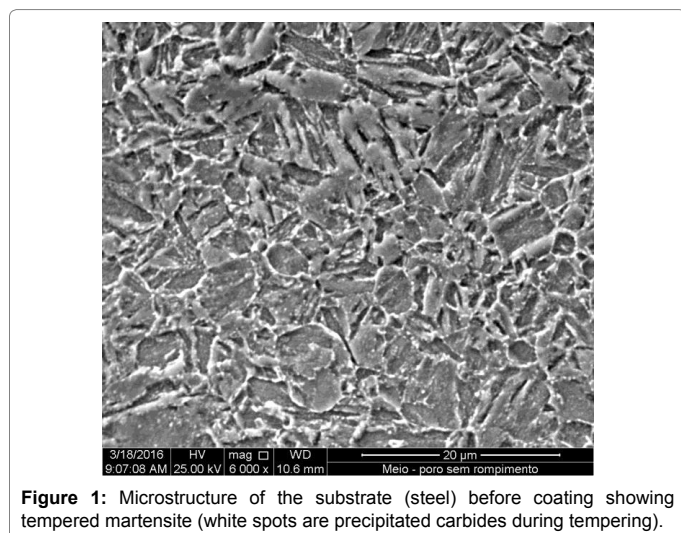
Microstructural characterizations were performed using light microscope and scanning electron microscope (SEM) integrated with energy-dispersive X-ray spectroscopy (EDX). Transversal cuts were done in order to investigate the cross section of the coating and interface coating/substrate (steel). The specimens were prepared by grinding down to 1200 mesh SiC paper followed by polishing in diamond paste of 1 μm and 0.5 μm size, respectively. Etching in Nital 2% was used to observe the substrate microstructure and electrolytic etching (current of 2 A and voltage of 10 V) with a solution of 10 vol % of oxalic acid ($C_2H_2O_4.2H_2O$) was used to observe the coating microstructure.

Vickers hardness measurement was done in order to evaluate the hardness profile along the cross section of the coating/substrate. The load was 1 kgf and the procedure is according to the standard ASTM E384-99.

Results and Discussion

The microstructure of the substrate (steel) observed in SEM after Nital 2% etching is as expected, that means, tempered martensite, as shown in Figure 1. The hardness test is, by far, the most valuable and most widely used mechanical test for evaluating the properties of metals as well as certain other materials. The hardness of a material usually is considered resistance to permanent indentation. In general, an indenter is pressed into the surface of the metal to be tested under a specific load for a definite time interval, and a measurement is made of the size or depth of the indentation. The principal purpose of the hardness test is to determine the suitability of a material for a given application, or the particular treatment to which the material has been subjected. The ease with which the hardness test can be made has made it the most common method of inspection for metals and alloys.

The general view of the coated samples is shown in Figure 2. The first three coatings were obtained by laser cladding and the last two coatings were obtained by thermal spraying technique.

Figure 3 shows the microhardness profile along the cross section of the coating/substrate. As it can be seen on Figures 3a and 3b, the microhardness of the laser coating based on Ni-super alloys (Haste alloy and Inconel 625), presented similar values (around 240-265 HV1), which are lower than the values presented by commercial alloys (e.g. Hasteallloy ~ 180HV10 and 295 HV10 for Inconel 625). This happens due to different microstructures: as-cast for the studied coatings and heat treated commercial alloys. Furthermore, some differences in chemical compositions as predictable. Additionally, in this study, it was used a load of 1 kgf, which is lower than for the comparison with the literature (10 kgf). Both of these coatings also presented microhardness not too far from the substrate, the substrate has a microhardness of around 220-230 HV1, which for many applications it is a positive characteristic. On the other hand, a peak of microhardness was observed in both coating/substrate systems. In case of the Haste alloy, the maximum microhardness measured was 452 HV1 and for the Inconel 625 it was measured 417 HV1. This feature might be not welcome for some industrial applications due to the presence of this so-called heat affected zone (HAZ) harder than the coating as well as the substrate.
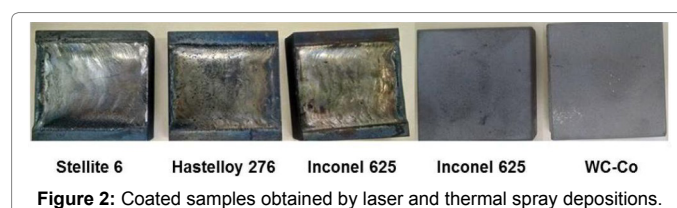
For the coating from the Co-based alloy (Stellite 6), the microhardness is much higher than those from Ni-based alloys; compare Figure 3c with Figures 3a and 3b. The microhardness measured for the coating Co-based alloy is in the range of the commercial Co-based alloy (392-458HV10). Similarly to the Ni-base coatings, the Co-base coating also presented a very hard heat affected zone (around 413 HV1).

For the coatings deposited by thermal spray process, the microhardness profiles are quite different from those obtained by laser cladding. Any HAZ was observed on both cases (Figures 3d and 3e), since an abrupt drop is observed at the coating/substrate interface. It is important to note, that when comparing Figure 3b (laser coating of Inconel 625) and Figure 3e (thermal spray coating of Inconel 625), it can be observed that the microhardness of the thermal spray coating is around two times higher than the coating Inconel 625 deposited by laser cladding, this is well explained by the completely different microstructural characteristics of both coatings.

For the coating composite W-C/Co-based alloy deposited by thermal spray, the microhardness also presented a very high value (around 1323 HV1) and absence of HAZ. In the literature, it is reported values in the range 1160-1300HV10 for this kind of coating. This magnitude of hardness might be of great advantage for applications on environment that imposes some kind of wear to the surface of the pipe.

The thickness of the laser coatings were around 2 mm and those obtained by thermal spray was around 650 μm for the Inconel 625 and around 670 μm for the composite W-C/Co-based alloy. Figure 4 shows a comparison of the two deposition processes in the case of Inconel 625.

The microstructures of the laser deposited coatings are similar to that classical as-cast microstructure during welding. Figure 5a shows the columnar grains in dendritic morphology with carbides (mainly
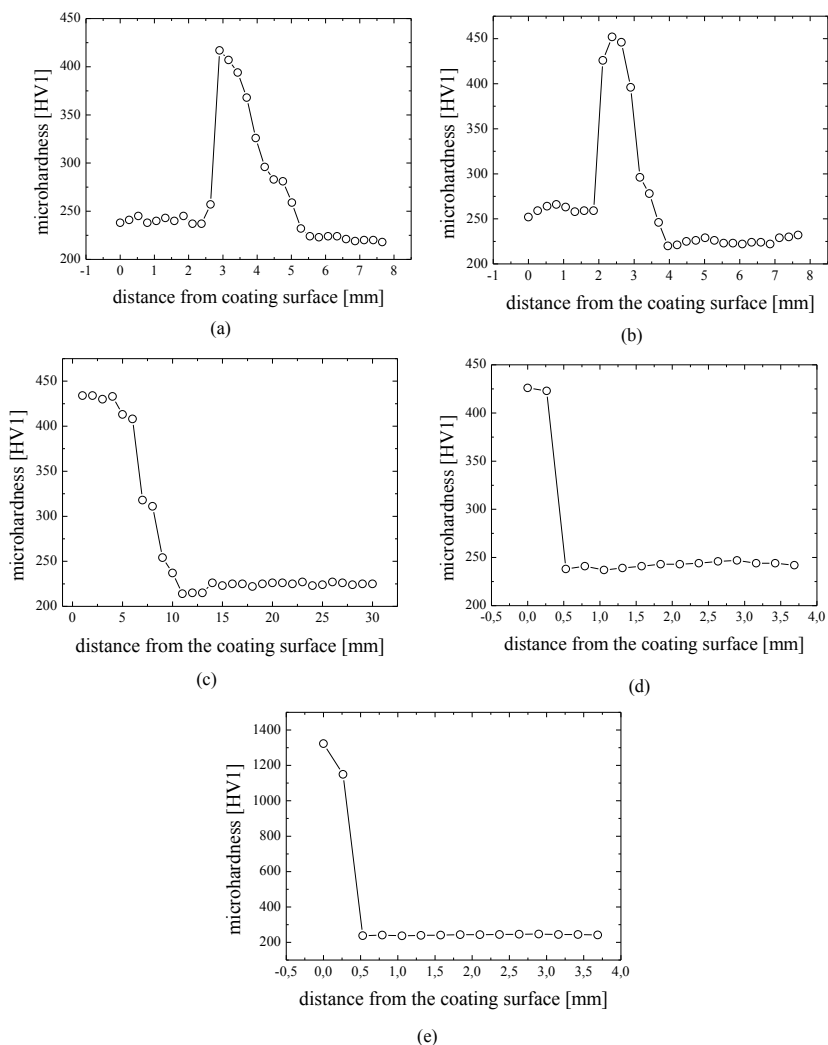

Figure 1: Microstructure of the substrate (steel) before coating showing tempered martensite (white spots are precipitated carbides during tempering).

Stellite 6   Hastelloy 276   Inconel 625   Inconel 625   WC-Co

Figure 2: Coated samples obtained by laser and thermal spray depositions.

Figure 3: Microhardness profile for the coated systems: (a) Inconel 625 laser coating, (b) Hastealloy laser coating, (c) Stellite 6 laser coating, (d) Inconel 625 laser coating and (e) composite W-C/Co-base alloy thermal spray coating.
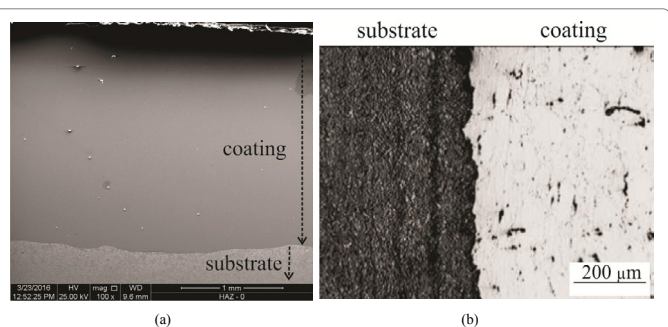

Figure 4: Cross section of the Inconel 625 coatings: (a) laser deposition and (b) thermal spray deposition.

Mo carbide) within the dendritic arms, it could also identify very fine Ti carbide (Figure 5b). Figure 5c shows the along the coating showing a thin dilution layer (the Fe profile) at the coating/substrate interface.

At the interface coating/substrate a thin dilution layer is formed on the laser coatings. Figure 6 shows this region with around 4-6 μm thickness layer. In the substrate, a wide HAZ of around 400 μm was observed in the case of laser deposition. Figure 7 shows an example of the HAZ for the case of Co-based alloy coating. It shows a gradient of grain size of the prior austenite, increasing from the substrate/coating interface to the substrate interior.

The major difference between the two deposition processes is the absence of HAZ for the cases of thermal spray depositions. Figure 8a shows that the microstructure close to the coating is modified in the case of laser deposition processes. It is observed the presence of martensite for the laser deposition (Figure 8a) processes and unchanged tempered martensite for the thermal spray processes (Figure 8b).

The presence of a HAZ with such high hardness for the case of laser depositions can be explained by the presence of a thermal gradient from the coating/substrate interface to the substrate interior (Figure 9). Generally, three different subzones within the HAZ could be observed. A first subzone with increasing in microhardness up to the maximum peak, this phenomena can be explained by the fully austenitization of the this region followed by martensite formation taking into account the very high hardenability of this steel (boron steel) and the high thermal gradient caused by laser process. The microhardness increases in the direction of the substrate because the austenite grain size decreases.
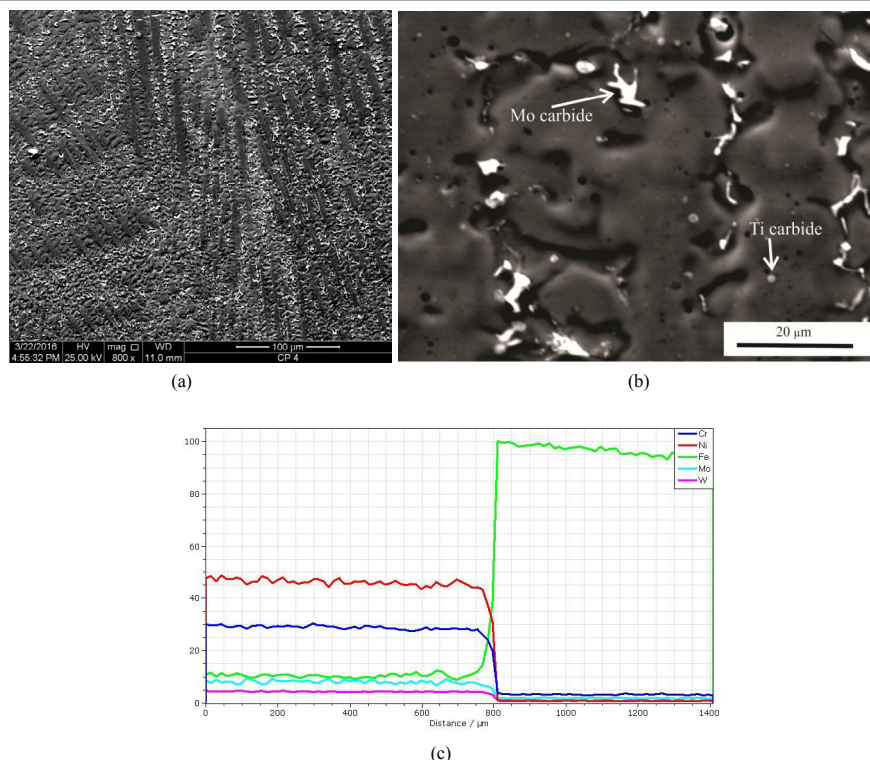
Figure 5: Typical microstructure of the laser coating of Ni-base alloys: (a) dentritic structure and (b) precipitate carbide and (c) EDS element profiles along the coating (distance from around middle of the coating).
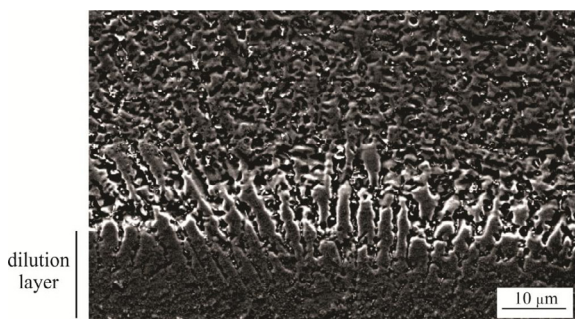

Figure 6: Formation of dilution layer on the laser coating/substrate interface in case of Inconel 625.

It is well known in the literature that the hardness of the martensite increases with decreasing austenite grain size [25-27]. The Ac_3 of this steel is 830°C and Ac_1 is 750°C measured using dilatometry. Therefore, the microhardness shall increase up to Ac_3. For the positions, where the temperature is below Ac_3, partial transformation of austenite occurred, and its amount decreases with decreasing in temperature until the Ac_1 is achieved (750°C) and consequently, the amount of martensite decreases, causing a continuous decreasing in microhardness. For the positions where the temperature is between 750°C and 650°C (the tempering temperature of the substrate is 650°C), the substrate is subject to a re-tempering, causing a decreasing of the hardness. Figure 3c, shows this profile quite clear, where the hardness drops below the hardness of the substrate.

Conclusion

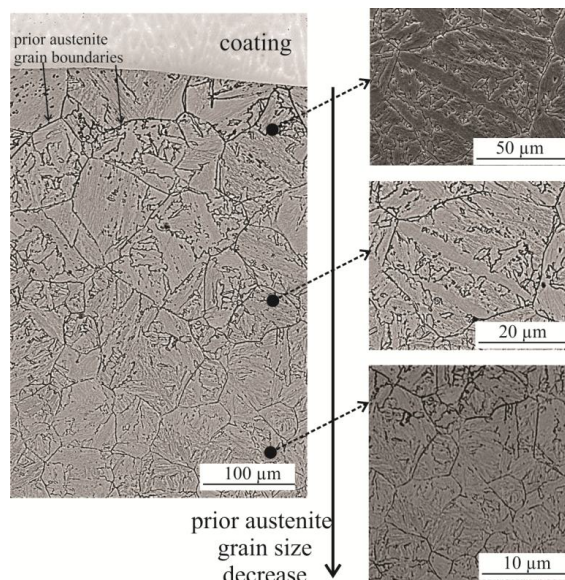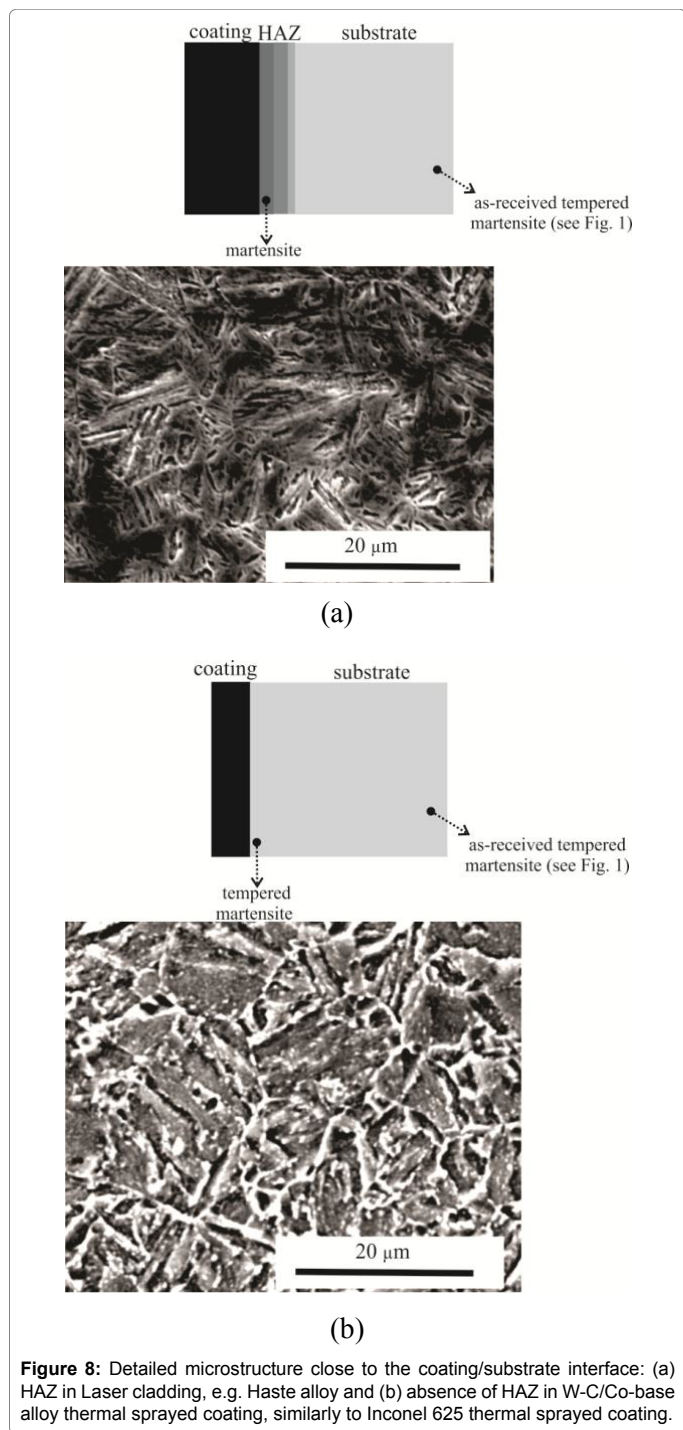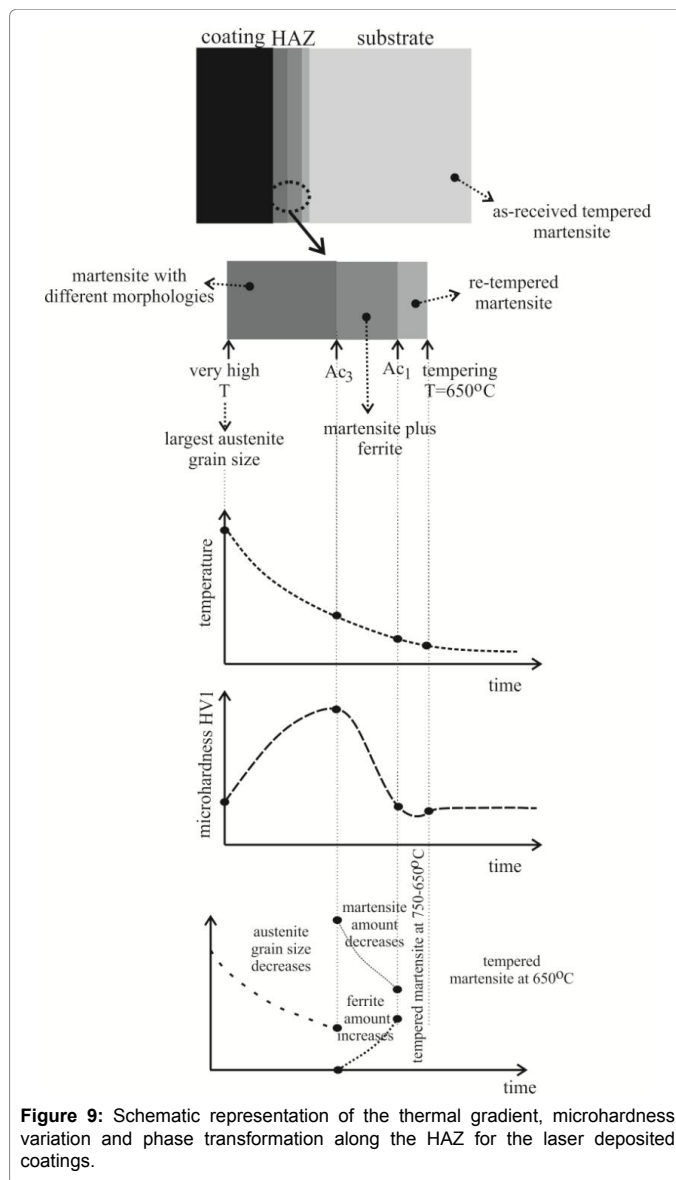Although there is a significant amount of studies of laser clad and

Figure 7: HAZ formed in the substrate during laser coating deposition (e.g. Co-based alloy).

thermal spray coating on steel substrate, this work was focused on a specific commercial API5CT grade L80 type 1 used for oil and gas industry. The following conclusions can be drawn the microhardness of the two Ni-based alloys deposited by laser cladding presented similar values to that of the steel substrate, which is beneficial for many applications. However, a hard HAZ was present, creating heterogeneity, which can be deleterious for some applications, e.g. sulfide stress corrosion. The Co-base alloy coating deposited by laser cladding

Figure 8: Detailed microstructure close to the coating/substrate interface: (a) HAZ in Laser cladding, e.g. Haste alloy and (b) absence of HAZ in W-C/Co-base alloy thermal sprayed coating, similarly to Inconel 625 thermal sprayed coating.

Figure 9: Schematic representation of the thermal gradient, microhardness variation and phase transformation along the HAZ for the laser deposited coatings.

presented higher hardness than those from Ni-based alloy. The coating hardness is in the same level as the hardness of the HAZ (approximately 430HV1). This higher hardness can be beneficial for applications subject to corrosion as well as wear environments. The alloy Inconel 625 and the composite W-C/Co-alloy deposited by thermal spray did not caused changing in the substrate that means there was no presence of HAZ. Besides that, the coating hardness is much very high, 430HV1 for Inconel 625 and approximately 1300HV1 for the composite W-C/Co-based alloy. These systems can be applied to the system requesting harsh wear resistance combined with corrosion resistance. A mechanism for the formation of HAZ in the laser coated systems was described. Prior austenite grain size was related to the morphology of transforming martensite, which influences the hardness profile in this region.

Acknowledgement

References

1. Joosten MW (2015) Corrosion of carbon steels by H_2S in CO_2 containing oilfield environments – 10 year update. Nace Corrosion Conference.

2. Lin T, Zhang Q, Lian Z, Liu Y (2016) Evaluation of casing integrity defects considering wear andcorrosion – application to casing design. Journal of Natural Gas Science and Engineering 29: 440-452.

3. Gao D, Sun L, Lian J (2010) Prediction of casing wear in extended-reach drilling. Petroleum Science 7: 494-501.

4. Rodriguez MALH, Delgado DIM, Gonzalez JR, Rodriguez J (2007) Corrosive wear failure analysis of a material gas pipeline. Wear 263: 567-571.

5. Kaldal GS, Jonsson M, Palsson H, Karlsdottir SN (2015) Structural modeling of the casings in high temperature geothermal wells. Geothermics 55: 126-137.

6. Olson DL, Siewert TA, Liu S, Edwards GR (1983) Welding, brazing and soldering. (9 Ed) Ohio, USA.

7. Marshall H (2007) Estates Gazette Law Reports. London, UK.

8. Zeng Y, Guzonas D (2015) Corrosion assessment of candidate materials for fuel cladding in Canadien SCWR. The Journal of the Minerals, Metals & Materials Society 68: 475-479.

9. Borgstedt HU (1966) Das Korrosionsverhalten der Nickelbasislegierung Inconel 625. Materials and Corrosion 17.

10. Ren F, Zhu W, Chu K (2016) Fabrication, tribological and corrosion behaviors of ultra-fine grained Co-28Cr-6Mo alloy for biomedical applications. Journal of the Mechanical Behavior of Biomedical Materials 60: 139-147.

11. Dinda GP, Dasgupta AK, Mazumder J (2009) Laser aided direct metal deposition of inconel 625 superalloy: Microstructural evolution and thermal stability. Material Science Engineering A 509: 98-104.

12. Altzinger UM, Ornig H, Schimboeuck R (1992) Hot rolled clad plates for application in flue gas desulfurization (FGD) – system. Materials and Corrosion 43.

13. Pajukoski H, Nakki J, Thieme S, Tuominen J, Nowotny S, et al. (2016) High performance corrosion resistant coatings by novel coaxial cold- and hot- wire laser cladding methods. Journal of Laser Applications 28.

14. Pontarrollo A, Vezzu S, Trentin A, Rech S, Guidolin M, et al. (2011) Characterisation of Inconel 625 coatings deposited by cold spray. International Thermal Spray Conference, Hamburg, Germany.

15. Michiels J (2006) Characterization and optimization of laser cladding inconel 625 alloy on A36 structural steel. Illinois Institute of Technology.

16. Abioye TE, McCartney DG, Clare AT (2016) Laser cladding of Inconel 625 wire for corrosion protection. Journal of Materials Processing Technology 217: 232-240.

17. Rajania HRZ, Mousavia SAAA, Sani FM (2012) Comparison of corrosion behavior between fusion cladded and explosive cladded inconel 625/plain carbon steel bimetal plates. Materials and Design 43: 467-474.

18. Paul CP, Gandhi BK, Bhargava P, Kukreja L (2014) Cobalt-free laser cladding on AISI type 316L stainless steel for improved cavitation and slurry erosion wear. Journal of Materials Engineering and Performance 23: 4463-4471.

19. Zhao XR, Zuo DW, Cheng H, Feng SS (2013) Microstructure and properties of laser cladding Co-based alloy layer. Advanced Materials Research 295-297.

20. Dawen Z, Maoquin W, Changsheng X (1998) Microstructural characteristics of a laser clad Co-base alloy. Rare Metal Materials Engineering 02.

21. Matos JF, Motta M, Antonini L, Malfatti C (2012) Abrasive wear resistance of API5L X65 steel coated with niobium plasma thermal spray and by inconel 625 welding. Dyna 79: 97-103.

22. Zhang D, Liu Y, Yin Y (2016) Preparation of plasma cladding gradient wear-resistant layer and study on its impact fatigue properties. Journal of Thermal Spray Technology 25: 535-545.

23. Bolelli G, Berger L, Bonetti M, Lusvarghi L (2014) Comparative study of the dry sliding wear behavior of HVOF-sprayed WC-(W,Cr)$_2$C-Ni and WC-CoCr hardmetal coatings. Wear 309: 96-111.

24. Venter AM, Oladijo OP, Luzin V, Cornish LA, Sacks N (2013) Performance characterization of metallic substrates coated by HVOF WC-Co. Thin Solid Films 549: 330-339.

25. Li X, Ma X, Subramanian SV, Shang C, Misra RDK (2014) Influence of prior austenite grain size on martensite-austenite constituent and toughness in the heat affected zone of 700MPa high strength line pipe steel. Materials Science & Engineering A 616: 141-147.

26. Kennett SC, Krauss G, Findley KO (2015) Prior austenite grain size and tempering effects on the dislocation density of low-C Nb-Ti microalloyed lath martensite. Scripta Materialia 107: 123-126.

27. Prawoto Y, Jasmawati N, Sumeru K (2012) Effect of prior austenite grain size on the morphology and mechanical properties of martensite in medium carbon steel. J Mater Sci Technol 28: 461-466.